Multiple Binding Modes of the Camptothecin Family to DNA Oligomers

Wojciech Bocian,*[a] Robert Kawęcki,[b] Elzbieta Bednarek,[a] Jerzy Sitkowski,[a, b] Agnieszka Pietrzyk,[b] Michael P. Williamson,[c] Poul Erik Hansen,[d] and Lech Kozerski*[a, b]

Abstract: The binding constants of camptothecin, topotecan and its lactone ring-opened carboxylate derivative to DNA octamers were measured by UV and NMR spectroscopy. The self-association of topotecan (TPT) was also measured. The carboxylate form of TPT binds in the same way as the lactone, but more weakly. Titration of TPT into $d(GCGATCGC)_2$ shows a preferred location stacked onto the terminal G1 base. However, the intermolecular NOEs cannot be reconciled with a single conformation of the complex, and suggest a model of a limited number of conformations in fast exchange. MD calculations on four pairs of starting structures with TPT stacked onto the G1–C8 base pair in different orientations were therefore performed. The use of selected experimental "docking" restraints yielded ten MD trajectories covering a wide conformational space. From a combination of calculated free energies, NOEs and chemical shifts, some of the structures produced could be eliminated, and it is concluded that the data are consistent with two major families of conformations in fast exchange. One of these is the conformation found in a crystal of a TPT/DNA/topoisomerase I ternary complex [*Proc. Natl. Acad. Sci. USA* **2002**, *99*, 15387–15392].

Keywords: alkaloids · antitumor agents · conformation analysis · docking · NMR spectroscopy

Introduction

A wealth of information from NMR studies on drug binding to DNA is now available.[1] The most detailed structural information is on intercalators, because their large association constants allow easy observation of intermolecular NOEs. Weaker ligands pose a much more difficult problem. The major source of structural restraints for these compounds is structure/activity relationships, and NMR input is largely limited to analysis of chemical shift changes, which have to date not been amenable to detailed structural interpretation.[2]

The cytotoxic plant alkaloid camptothecin (CPT) and a synthetic derivative, topotecan (TPT), have emerged as clinically useful anticancer drugs,[3] but are of this difficult, weakly binding, type. They act as inhibitors of topoisomerase I (TopoI)[4] through the formation of stable ternary complexes composed of the drug, DNA and TopoI.[4a–c] An im-

[a] Dr. W. Bocian, Dr. E. Bednarek, J. Sitkowski, Prof. Dr. L. Kozerski
National Institute of Public Health
00-725 Warszawa, Chełmska 30/34 (Poland)
Fax: (+48) 228-410-652
E-mail: lkoz@icho.edu.pl
lkoz@il.waw.pl

[b] Dr. R. Kawęcki, J. Sitkowski, A. Pietrzyk, Prof. Dr. L. Kozerski
Institute of Organic Chemistry, Polish Academy of Sciences
01-224 Warszawa, Kasprzaka 44 (Poland)
Fax: (+48) 226-326-681

[c] Prof. Dr. M. P. Williamson
Department of Molecular Biology and Biotechnology, University of Sheffield, Sheffield S10 2TN (UK)
E-mail: m.Williamson@sheffield.ac.uk

[d] Prof. Dr. P. E. Hansen
Department of Life Sciences and Chemistry
Roskilde University, 4000 Roskilde (Denmark)
E-mail: poulerik@ruc.dk

Supporting information for this article is available on the WWW under http://www.chemeurj.org/ or from the author: Table S1 gives the fitted diffusion coefficients for the studied chemical shift dependence on the gradient strength in the diffusion experiment, Table S2 gives the ^{1}H NMR chemical shifts of free $d(GCGATCGC)_2$, Tables S3 and S4 give the ^{1}H NMR chemical shifts of $d(GCGATCGC)_2$ in the presence of topotecan (TPT), Table S5 gives the ^{1}H T_1 relaxation times of $d(GCGTACGC)_2$ in D_2O, Figure S1 shows a binding isotherm of TPT to $d(GCGATCGC)_2$ established by UV, Figure S2 shows a graph of the chemical shift changes on titration of $d(GCGATCGC)_2$ with TPT 1:1 at 13 °C, pH 6 (sample 1), Figure S3 shows a graph of the chemical shift changes on titration of $d(GCGATCGC)_2$ with TPT 1:1 at 30 °C, pH 6 (sample 2), and Figure S4 shows the aliphatic part of a NOESY spectrum of the complex with TPT, with some intermolecular NOEs indicated.

DOI: 10.1002/chem.200305624

portant feature of the binding interaction is the lactone functionality of TPT, which hydrolyses to the ring-opened carboxylate form in a pH-dependent manner (Scheme 1), being >80% ring-opened at pH 7.4.[4e,f,h] Most biological

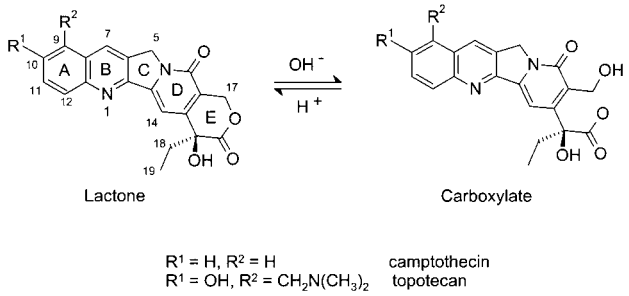

Scheme 1. pH-dependent hydrolysis of the TPT lactone functionality to the ring-opened carboxylate form.

assays indicate that the carboxylate form of TPT is inactive as a TopoI inhibitor. Structure/function relationships have been analysed,[4f,5] and structures have been described.[6] The enzyme forms a "clamp" around a nicked B-form DNA. TPT intercalates, stacking with its long axis parallel to GC(+1).

Two recent NMR studies give some preliminary information concerning interactions of TPT with short DNA oligomers[7] and *ss* or *ds* polynucleotides.[8] However, the mode of TPT binding to DNA was not systematically studied, and the role of the carboxylate form of TPT was not fully recognized. We have therefore been studying binding of the CPT family to DNA oligomers, and show here that the data are not consistent with binding in a single geometry. We present a novel combination of experimental and theoretical methods, demonstrating that two major conformations exist. One of these is similar to that seen in a ternary complex,[6a] but the second is previously uncharacterized. This result may be of relevance to the design of novel antitumor agents based on the camptothecin family.

Results and Discussion

TPT self-association constant:[9] Before DNA binding could be analysed, self-association of CPT or TPT had to be studied. TPT self-association was analysed by NMR by use of the isodesmic model (see Experimental Section).[10] The results of the fit are given in Table 1, and the binding isotherm is shown in Figure 1. All protons are shifted to lower frequencies in the self-associated state, consistently with the expected stacked structure. The self-association constant derived from the data is $3.4 \pm 1.0 \times 10^3\,\text{M}^{-1}$, in agreement with a recent measurement.[11]

DNA/TPT binding constant measurements: The binding constant of TPT to DNA was measured by UV, by use of equations corrected for TPT self-association as described in the Experimental Section. The binding constant of TPT with $d(GCGATCGC)_2$ was obtained as $K_a = 2.5\,\text{mM}^{-1}$ (K_d =

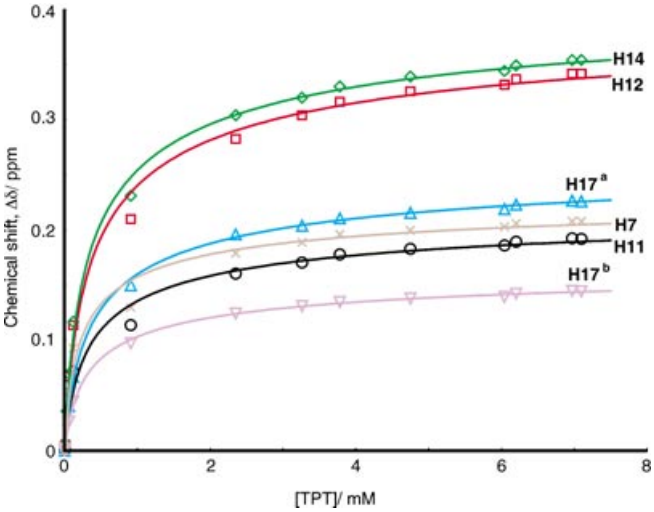

Figure 1. Self-association isotherm of TPT in phosphate buffer (pH 6, 30°C).

Table 1. Data for the evaluation of the self-association constant (K_a^{TPT}) of TPT from dilution experiments (30°C, pH 6).

Proton	δ_{mon} [ppm][a]	$\Delta\delta_{max}$ [ppm][a]	K_a^{TPT} [M^{-1}] $\times 10^3$
H7	8.804	0.240	5.4
H12	8.222	0.419	2.8
H11	7.649	0.233	3.2
H14	7.675	0.431	3.1
H17a	5.678	0.281	2.7
H17b	5.492	0.177	3.0

[a] The experimentally determined values for the monomer (δ_{mon}) were established at very low (5 μM) concentrations and $\Delta\delta_{max}$ obtained from iterative fitting of the concentration dependence of the chemical shifts.

0.4 mM) at 24°C and pH 5.0 (100% of the lactone form). The binding isotherm is shown in the Supporting Information.

NMR determination of DNA/campthotecin family binding constants: Two types of NMR experiment were used to study binding of the CPT family of drugs to DNA: measurements of the diffusion coefficients of CPT alone and in the presence of DNA, and titration of buffered DNA with TPT. Double-stranded DNA duplexes $d(GCGTACGC)_2$ and $d(GCGATCGC)_2$ were used in pulsed field gradient experiments with CPT and in titration experiments with TPT, respectively.

CPT/DNA binding constant: The PGSE experiment is especially appropriate for measuring weak binding of a molecule of low molecular weight, such as CPT (M_W = 311 Da), to a molecule of much higher molecular weight (DNA, $M_W \approx$ 2.8 kDa), because the diffusion constant for bound CPT is the weighted average of the diffusion constant for free CPT and the diffusion constant for DNA, which allows calculation of the ratio of free to bound CPT and thus of the association constant. Applications of the method to solute binding have recently been reviewed.[12]

Figure 2 shows a PGSE plot of CPT in the presence of $d(GCGTACGC)_2$. By published procedures,[13] the binding

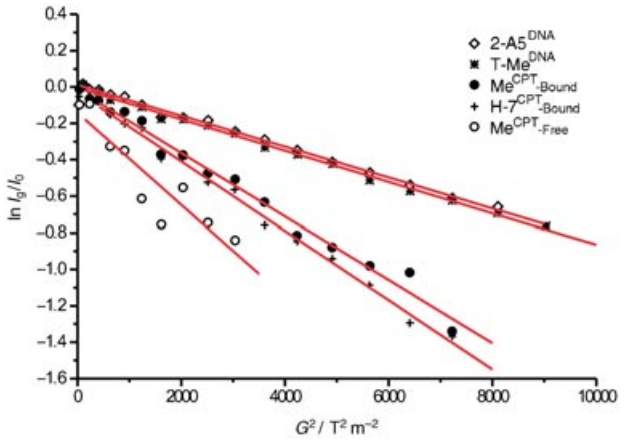

Figure 2. 1D Pulsed field gradient diffusion experiment, in which the slope of the graph is proportional to the diffusion constant. Semilogarithmic plot of signal intensity against the square of the gradient strength, showing different diffusion constants for DNA, bound CPT and free CPT (same buffer and concentration).

constant for CPT to the d(GCGTACGC)$_2$ duplex was obtained as $K_a = 1.7\,\mathrm{mM}^{-1}$ ($K_d = 0.6\,\mathrm{mM}$) at pH 6.0.

TPT/DNA binding constant: Shift changes observed on titration of d(GCGATCGC)$_2$ with TPT are mostly upfield, and are largest on the terminal G1–C8 base pair. Some chemical shift changes in C8 are downfield (see Figure 6 and Supporting Information), which implies stacking of TPT to the end of the DNA stem in a restricted geometry. The largest shift change is of the imine resonance of G1 (ca. −0.4 ppm), which is not surprising as it is in the centre of the base pair. A single set of resonances is observed for each component, and the C_2 symmetry of the DNA duplex is maintained, the drug hence being in fast exchange with DNA. In order to check the significance of measured shifts we studied the chemical shift dependence on dilution, temperature and pH changes. Dilution by 20% does not influence the DNA resonances, which remain constant to ±0.005 ppm. A change of pH from 7 to 6 changes the position of resonances uniformly, on average by 0.15 ppm to higher frequencies. Raising the temperature makes the chemical shift changes less specific (Supporting Information), in that changes in the middle of the DNA stem increase relative to changes at the end. This is presumably due to a reduction in the specificity of binding at higher temperature.

The DNA/TPT dissociation constant K_d was obtained by NMR titration, as described in the Experimental Section, to give $K_d = 0.7 \pm 0.2\,\mathrm{mM}$ ($K_a = 1.4 \pm 0.3\,\mathrm{mM}^{-1}$) and $K_a^{DNA} = 0.4 \pm 0.4\,\mathrm{mM}^{-1}$ at 30 °C, pH 6.0 and 0.1 mM TPT concentration (Table 2, Figure 3). The errors are estimated as the sum of standard deviation and systematic errors derived from imprecision of DNA concentration, measured as the sum of dilution steps. The latter error has an especially high influence on the K_a^{DNA} value.

Table 2. Equilibrium constants relevant to the DNA/TPT interaction.[a]

Proton	K_d [mM]	K_a [mM^{-1}]	K_a^{TPT} [mM^{-1}]	K_a^{DNA} [mM^{-1}]	$\Delta\delta_{max}$ [ppm]	$\Delta\delta_{max}^{corr}$ [ppm]
H11	0.77	1.30	3.15	0.57	0.525	0.233
H12	0.87	1.15	2.82	0.53	0.518	0.419
H7	0.69	1.45	5.44	0.45	0.382	0.240
C9-CH$_2$[b]	0.58	1.72	3.38	0.22	0.296	0.234
H11[c]	0.80	1.25	0	0.60	0.558	
H11[d]	0.75	1.33	0	0	0.461	

[a] See Equations (8)–(12) for the meaning of the constants. K_a is defined as $1/K_d$. The $\Delta\delta_{max}^{corr}$ value accounts for the shift due to TPT association. [b] Negligible chemical shift nonequivalence was observed between the geminal protons, which are treated throughout the work as a single signal. [c] The values given for K_d and K_a refer to calculated constants assuming the $K_a^{TPT} = 0$. [d] The values given for K_d and K_a refer to calculated constants assuming $K_a^{TPT} = 0$ and $K_a^{DNA} = 0$.

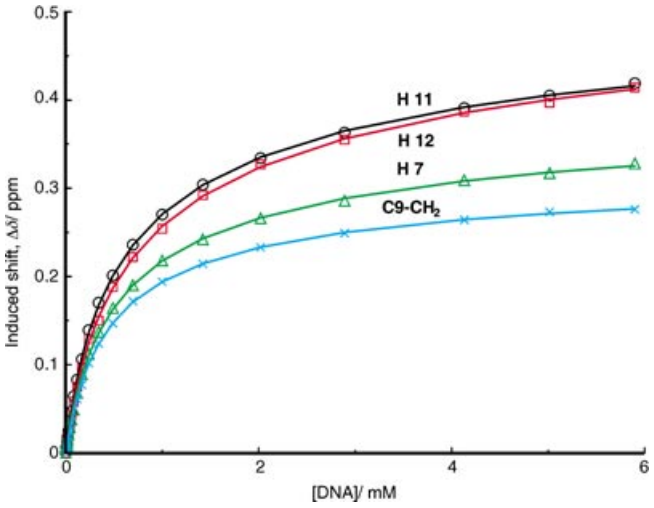

Figure 3. Binding isotherm of d(GCGATCGC)$_2$ DNA duplex interaction with the lactone form of TPT at pH 6, 30 °C.

The precision of our NMR experiment is much higher than that of the UV experiment, but nevertheless, the similarity of this binding constant to that determined by UV increases our confidence in its absolute value. As shown in the Supporting Information (Figure S1), the changes in UV absorbance in the concentration range studied are very small.

TPT carboxylate/DNA binding: At physiological pH, TPT exists in both the lactone and the carboxylate anion forms, although the lactone form may be stabilized by the presence of DNA.[7] It is therefore important to evaluate the binding of the carboxylate form to DNA. In NMR titrations, the chemical shifts of the carboxylate form change upon addition of DNA oligomers (Table 3). The pattern of the shift changes, although limited, is similar to that seen for the lactone, consistently with binding in a similar geometry (a result at variance with a recent NMR investigation of the linewidths of both forms in the presence of poly ss and poly ds nucleotides).[8] The chemical shift changes suggest that binding of the carboxylate is weaker than that of the

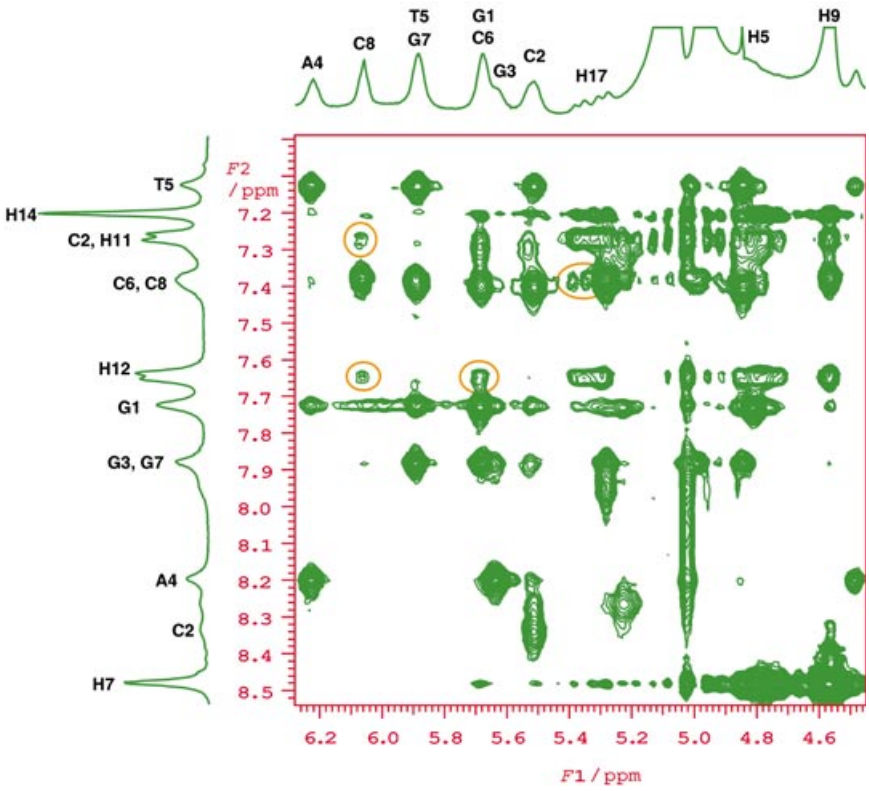

Figure 4. Example of one of the processed NOESY spectra of d(GCGATCGC)$_2$ in the presence of TPT (3 °C, TPT/DNA ratio 2.5:1, pH 5.0). Signals marked in ellipses indicate considered examples of intermolecular cross-peaks between TPT and DNA.

Table 3. TPT lactone and carboxylate form chemical shifts for isolated TPT, together with changes in the presence of ds DNA oligomers (in brackets).

Form	H7	H11	H12	H14	pH
lactone[a]	8.66	7.53	8.04	7.50	6.0
	(−0.15)	(−0.20)	(−0.18)	(−0.11)	
lactone[a]	8.29	7.31	7.48	7.34	7.25
	(+0.07)	(−0.10)	(−0.17)	(−0.06)	
lactone[b]	8.41	7.40	7.91	7.38	6.28
	(≈0)	(≈−0.05)	(>−0.1)	(≈−0.05)	
lactone[c]	8.62	7.43	7.87	7.3	7.0
	(−0.07)	(−0.19)	(−0.14)	(+0.10)	
carboxylate[d]	8.38	7.33	7.91	7.58	7.25
	(−0.01)	(−0.07)	(−0.10)	(−0.05)	
carboxylate[e]	8.45	7.41	7.98	7.60	6.28

[a] This work. Values in brackets indicate change with octamer d(GCGATCGC)$_2$, 1:1 DNA/TPT ratio. [b] From ref. [8], changes refer to interaction with poly ss(dA). Interaction with poly ss(dT) results in appreciable high-frequency shifts (not cited) for H7, H11 and H14, but no shift for H12. [c] From ref. [7], changes refer to interaction with hexamer d(CGTACG)$_2$. [d] This work. Changes with d(GCGATCGC)$_2$, 1:1 lactone/carboxylate ratio. [e] From ref. [8]. Changes on interaction with poly ss or poly ds not cited.

lactone, but do not allow us to fit a K_d value. We therefore analysed binding by fluorescence spectroscopy of DNA/TPT mixtures at pH 6.3 (lactone) and 7.8 (carboxylate). At pH 6.3, the emission peak on excitation of the TPT 382 nm band was quenched by 6.5% on addition of DNA. No quenching of the TPT fluorescence was observed at pH 7.8. The lack of quenching implies that binding of the carboxylate is weak, in line with its lack of biological activity, but contrary to conclusions from the ternary complex structure,[6a] which showed that the carboxylate form can be equally well accommodated in an intercalation pocket in an enzymatically prepared nick structure and has even better stabilisation from close enzyme units than the lactone.

The DNA/TPT binding mode

Experimental restraints: At a 2.5:1 TPT/DNA ratio, the drug is still in fast exchange, but for the first time it is possible to observe cross-peaks due to NOE effects between TPT and DNA (Figure 4). These involve the protons shown in Table 4, and are not consistent with a single geometry of the complex. Some others are also anticipated from molecular modelling (indicated with question marks in Table 4) but were not used in this study due to overlap. Some of these cross-peaks persist, with lowered intensities, if the temperature is raised to 13 °C, which confirms their intermolecular origin, since the change in intensity parallels the change in concentration of the complex. In general these cross-peaks are much weaker than the intramolecular DNA or TPT cross-peaks. Similarly to what was seen with the chemical shift changes, the cross-peaks are observed at the edge of the duplex but not in the centre of the stem. These experiments strongly suggest that the G1 base, located at the edge of the duplex, is the predominant site of TPT binding, consistently with spectrophotometric studies.[14] However, our studies suggest that the interaction is one of stacking against a base pair rather than an interaction with the minor groove.[11]

An issue that should be addressed in drug–DNA interactions is the possibility of spin diffusion as a source of indirect cross-peaks.[15] A good indicator of spin diffusion is the presence of multiple cross-peaks involving a network of adjacent nuclei, and these are not observed. Thus, no cross-peaks from H7 and H14 of TPT to DNA were observed, except for very weak responses to H8–G1, although both protons give well resolved separate singlet resonances and

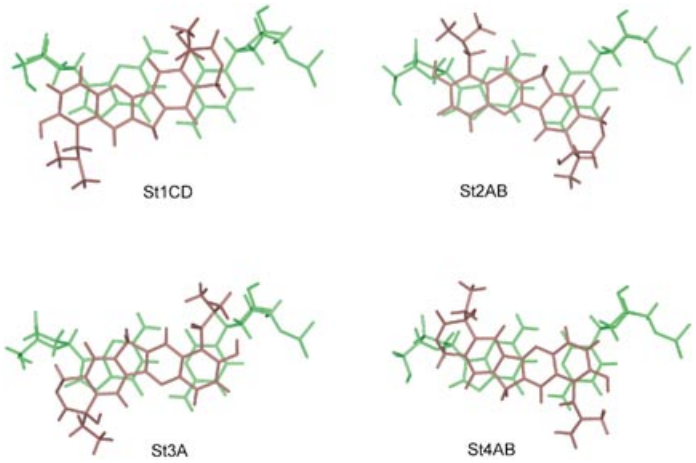

Figure 5. Average geometries derived from MD trajectories for selected structures of the TPT/d(GCGA)$_2$ complexes, showing TPT stacked over the G1-C8 base pair.

are therefore easy for spectral analysis. Similarly, only the DNA resonances facing the TPT molecule give cross-peaks: H2′ and H2″ of G1 or C2, for example, do not give cross-peaks, whereas strong cross-peaks to H1′, H3′ and H4′ of G1 are observed. Spin diffusion is therefore unlikely to be responsible for significant NOE intensity in our spectra.

A further complication is that, irrespective of the temperature of the measurements, aggregation of TPT is observed in the sample with 2.5 times TPT molar excess. This is evidenced by NOE effects—H12–H7 or H11–H7, for example—that cannot be intramolecular and can arise only from intermolecular contacts. These cross-peaks diminish in intensity with increasing temperature but are observed at all three temperatures (3, 13 and 30 °C).

Molecular modelling: Modelling studies of DNA interactions with the CPT family have been published.[16] However, our approach is necessarily different, because the experimentally observed data demonstrate multiple binding modes in fast exchange. It is therefore necessary to adopt an unconventional approach. Rather than assume a single conformation and restrain it with all the experimentally observed NOEs, here we assume from the outset that several conformations are present in fast exchange, implying that the complete set of experimentally observed NOEs cannot be satisfied simultaneously. Therefore, we use only one or two experimentally derived "docking" NOEs to maintain TPT close to the oligonucleotide, and only compare the resultant structures to the NOE and chemical shift restraints afterwards. In this way we avoid biasing the calculation by inclusion of internally inconsistent NOE values.

As starting conformations, four possible stacking alignments of TPT along the terminal GC units were used (Scheme 2). Molecular dynamics simulations were performed over a nanosecond timescale, with back-calculations of NOE and chemical shift effects, with the aim of determining the most significant contributing conformations. It is well known that suitable reproduction of NOE effects requires good coverage of conformational space. This turns out to be very difficult for big molecules and even worse when an intermolecular interaction is considered.[17] To minimize computational time we have used only the first four base pairs of our DNA octamer

Table 4. NMR-derived and MD back-calculated NOE effects for selected structures.[a]

Experimental				TPT			
DNA	C9-CH_2	NMe	H11	H12	18-CH_2	19-CH_3	17-CH_2
H8G1	○	○	○	○		?	○
H1′G1	●	●	○	○	●	●	●
H3′G1		○				○	?
H4′G1	○	●	○	?	●	●	●
H5′,H5″G1	○	○	○	○	○	○	●
H1′C2		○				○	
H4′C2		●			○	●	
H5′,H5-C2	?	●			○	●	
H6C8	?	○	○	?	○	○	●
H1′C8	?	○	○	○		○	?
H2′,H2″C8	?	○	●	●		○	○
St 1CD				**TPT**			
DNA	C9-CH_2	NMe	H11	H12	18-CH_2	19-CH_3	17-CH_2
H8G1	○	○	○	○			
H1′G1			○	○			
H3′G1			○				
H4′G1	○		○	○			
H5′,H5″G1	○	○	●	●			
H1′C2							
H4′C2							
H5′,H5″C2							
H6C8							○
H1′C8						○	○
H2′,H2″C8						○	●
St 2AB				**TPT**			
DNA	C9-CH_2	NMe	H11	H12	18-CH_2	19-CH_3	17-CH_2
H8G1	○	○	○	○			
H1′G1	●	●	○	○			
H3′G1		○					
H4′G1	○	●	○				
H5′,H5″G1	○	○	○				
H1′C2		○					
H4′C2		●					
H5′,H5-C2	○	●					
H6C8					○	○	●
H1′C8							○
H2′,H2″C8							●

Table 4. (Continued)

St 3A DNA	TPT C9-CH_2	NMe	H11	H12	18-CH_2	19-CH_3	17-CH_2
H8G1						○	○
H1′G1							○
H3′G1							○
H4′G1							○
H5′,H5″G1							●
H1′C2		○					
H4′C2							
H5′,H5″C2							
H6C8	○	○	○	○			
H1′C8	○	●	○				
H2′,H2″C8	●	●	○				

St 4AB DNA	TPT C9-CH_2	NMe	H11	H12	18-CH_2	19-CH_3	17-CH_2
H8G1							○
H1′G1					●	●	●
H3′G1						○	
H4′G1					●	●	●
H5′,H5″G1					○	○	●
H1′C2						○	
H4′C2					○	●	
H5′,H5″C2					○	●	
H6C8	○	●	○	○			
H1′C8		○	○	○		●	
H2′,H2″C8	○	○	●	●		○	

[a] ● and ○ denote large and small NOE effects, respectively. In the case of back-calculated NOE, "large" means more than 15% of the reference H5–H6 cytosine NOE, and "small" means more than 1% and less than 15% of the H5–H6 NOE. ? indicates that presence of the corresponding cross-peak in NOESY spectra cannot be confirmed, mostly because of overlapping signals. In the case of CH_2 groups (C9-CH_2, 17-CH_2, 18-CH_2, H5′, H5″, H2′, H2″) and CH_3 groups (19-CH_3, NMe) the sum of the NOEs was calculated.

$[d(GCGA)_2]$ in simulations, with restraints holding the last AT base pair atoms in their initial X-ray-derived positions. We believe that this simplified model is adequate, because, as our results show, only the terminal GC unit directly interacts with TPT. A separate issue is correct docking of TPT. During our initial studies (1 ns MD equilibration of the starting complexes) we determined that the starting configuration of TPT in the complex is very important, especially when MD time is limited. In particular, proper docking was only obtained for St3 in the initial calculations, and so, after equilibration, we applied an additional re-docking procedure for complexes St1, St2 and St4 (see Experimental Section). Each trajectory was repeated with the other possible starting orientation of the -CH_2-NMe_2 group (bent into or away from the DNA). This intervention was necessary because of a high energy barrier for rotation about its dihedral angle. During our 600 ps production MD simulations we observed only a limited number of spontaneous crossings to the opposite orientation of the -CH_2-NMe_2 group, usually not more than one (if any) per trajectory. The restraints used, and key results, are listed in Table 4.

Since we are dealing with a multiconformation approach, the criteria for choosing successful structures are crucial. This is primarily achieved by examining free energy differences between structures. The calculated mean free energies for the simulated complexes are listed in Table 5.

The computed total free energy changes are generally small, of the order of a few kcal mol^{-1}. The least stable are adducts derived from the initial structure St1, while St2, St3 and St4 are of similar stability. The largest contribution to the free energy differences is the gas-phase electrostatic energy E_{elec}, which is mostly responsible for the attractive interactions between ligand and receptor.[18] This favours the complex St2B (the lowest E_{elec}) over St1B (the highest E_{elec}) by 23 kcal mol^{-1}, while the electrostatic solvation energy G_{PB}, the second largest contribution to the free energy changes, favours St1B over ST2B by 11 kcal mol^{-1}. The absolutely most stable complex St3B (i.e., the lowest ΔG_{tot}) owes its stability over St2B mostly to a 3.3 kcal mol^{-1} lower internal energy (E_{int}). The van der Waals energy (E_{vdW}) and nonpolar term of the solvation free energy (G_{npol}) (the solvent-accessible surface area-dependent term) make only small contributions to the total free energy changes, of less than

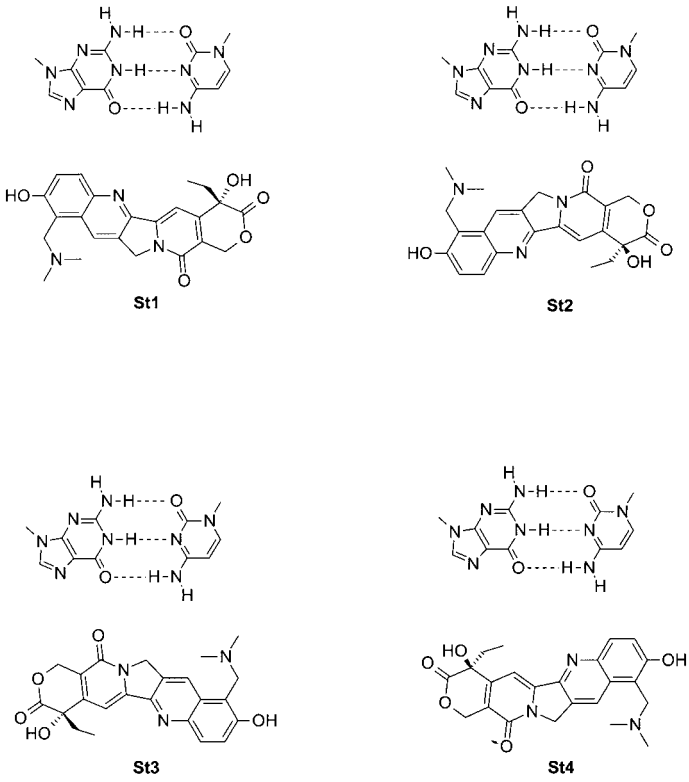

Scheme 2. Schematic representation of the stacking interactions of TPT with the terminal base pair in the DNA octamer $d(GCGATCGC)_2$ in four starting geometries used in MD calculations.

Table 5. Docking parameters and free energy analysis for simulated adducts.

Structure[a]	Docking restraints	Initial orient. of -NMe_2 group	Average energies [kcal mol^{-1}][b]								
			$\langle E_{elec}\rangle$	$\langle E_{int}\rangle$	$\langle E_{vdW}\rangle$	$\langle E_{MM}\rangle$	$\langle G_{npol}\rangle$	$\langle G_{PB}\rangle$	$\langle G_{solv}\rangle$	$\langle G_{tot}\rangle$	ΔG_{tot}
St1A	H12-TPT/H1′G1	outward	162.0	429.3	−143.1	448.2	12.4	−924.5	−912.2	−463.8	0
			(12.8)	(12.4)	(5.3)	(19.3)	(0.1)	(5.0)	(5.0)	(17.2)	
St1B	H12-TPT/H1′G1	inward	168.8	427.7	−143.9	452.6	12.3	−925.1	−912.8	−460.2	3.6
			(12.2)	(12.4)	(4.5)	(18.2)	(0.1)	(4.8)	(4.8)	(17.6)	
St1C	H12-TPT/H8-G1	outward	160.7	429.3	−143.6	446.3	12.3	−923.3	−911.0	−464.6	−0.8
			(12.3)	(14.1)	(4.8)	(17.1)	(0.1)	(5.0)	(5.0)	(16.3)	
St1D	H12-TPT/H8-G1	inward	159.9	427.8	−143.4	444.3	12.4	−922.8	−910.4	−466.1	−2.3
			(10.0)	(11.1)	(4.1)	(14.8)	(0.1)	(4.7)	(4.6)	(13.8)	
St2A[c]	H12-TPT/H1′G1	outward	148.6	425.2	−143.8	430.0	12.2	−914.6	−902.3	−472.3	−8.5
			(10.5)	(11.8)	(4.9)	(16.4)	(0.2)	(4.8)	(4.7)	(14.6)	
St2B[c]	H12-TPT/H1′G1	inward	145.8	426.5	−143.0	429.3	12.3	−914.1	−901.8	−472.5	−8.7
			(10.3)	(12.2)	(5.1)	(16.8)	(0.2)	(4.3)	(4.3)	(15.5)	
St3A[c]	no restraints	outward	152.3	423.2	−144.0	431.5	12.2	−916.9	−904.7	−473.2	−9.4
			(10.1)	(11.7)	(4.8)	(15.9)	(0.1)	(4.5)	(4.5)	(15.5)	
St3B	no restraints	inward	155.5	424.9	−143.6	436.8	12.2	−917.3	−905.1	−468.3	−4.5
			(12.7)	(12.1)	(4.2)	(19.0)	(0.1)	(5.0)	(4.9)	(16.8)	
St4A[c]	19-CH_3 TPT/H5′,5″G1-C2	outward	149.8	427.2	−143.4	433.6	12.2	−917.5	−905.3	−471.7	−7.9
			(10.8)	(12.2)	(4.6)	(19.2)	(0.1)	(4.1)	(4.1)	(17.6)	
St4B[c]	19-CH_3 TPT/H5′,5″G1-C2	inward	150.5	427.1	−143.5	434.0	12.2	−916.4	−904.3	−470.2	−6.4
			(10.2)	(13.0)	(4.6)	(19.1)	(0.2)	(4.5)	(4.4)	(18.0)	

[a] See Scheme 2. [b] Values in parentheses are standard deviations. ΔG_{tot} are relative to St1A. [c] See Figure 5.

1 kcal mol^{-1}, implying that in our weakly bonded complexes neither the van der Waals interaction nor the solvent-accessible surfaces make it possible to distinguish different conformations in the ligand–receptor interactions.

A comparison of experimentally derived NOE cross-peaks with back-calculated NOE effects derived from MD trajectories is reported in Table 4. The calculated NOE effects are presented as averages over inward and outward -CH_2-NMe_2 geometries for starting structures St1, St2 and St4. This was performed in order to probe the conformational space more thoroughly. For St1 we have analysed trajectories C and D instead of A and B, because they have lower free energies, while for St3 we report only trajectory A, because trajectory B has a much higher free energy. Tables 4 and 6 show all those intermolecular effects that could be unambiguously assigned. Expected but overlapped cross-peaks are either not taken into account or are marked with a question mark in the tables. Empty spaces in the tables mean that the cross-peaks are not observed. It is important to note that there are almost no unused calculated NOE effects for any of the investigated structures (the exception is one weak unexpected NOE effect between H3′G1 (DNA) and H11 (TPT) in St1 CD). Table 4 does not allow us automatically to exclude any of our structures as definitely wrong or of minor significance on the basis of observed matching of the experimentally observed and the calculated NOEs. Similarly, a simple analysis of the number of predicted NOE effects is not very helpful. The fact that for none of the individual structures does the number of predicted effects exceed 50 % of the observed effects does not necessarily mean that they are wrong, rather this clearly indicates that we have to explore a multi-conformational model, of which the simplest is a model considering averaging between pairs of structures.[19] In this model we cannot in advance anticipate the participation of each structure, and so we cannot exclude any of them only on the basis of match of predicted NOE effects.

Table 6 gives the results of back-calculations of NOE effects for the averages of pairs of selected conformations, and Figure 5 displays the geometries for these structures.

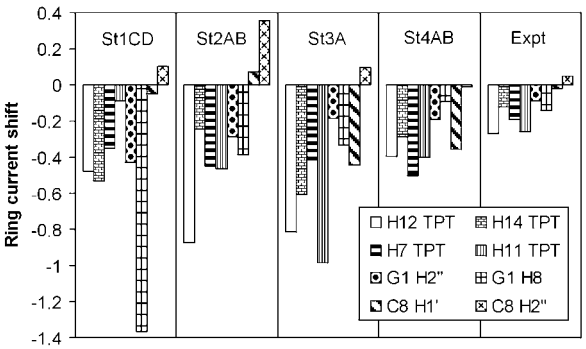

Figure 6. Experimentally observed chemical shift changes (ppm) on titration of TPT into d(GCGATCGC)$_2$; 1:1 TPT/DNA molar ratio at 3 °C, pH 6 in D_2O, compared for each of the four starting structures. Shifts are shown for four signals from the terminal base pairs (symmetry-related signals from both strands retain identical shifts) and for four protons from TPT.

The conformations were selected on the basis of free energy and complementarities in NOE effect patterns. The averages were calculated for equal concentrations of each structure. The calculation is not sensitive to exact ratios of concentration, because the NOE effects are much more dependent on the geometry (r^{-6} dependence) than on concentration. This analysis shows an almost perfect match of experimentally observed to calculated NOE effects for the 1:1 average of structures St2AB and St4AB. Although we observe this very good correlation for combination St2 + St4, we cannot definitely exclude the remaining combinations. In particular, the lowest-energy St3A may participate in the interactions, but we cannot confirm or exclude this from the NOE data.

We therefore carried out an analysis of chemical shift effects, induced by ring current effects in the TPT/octamer

Table 6. NMR-derived and back-calculated total NOE effects for equal combination of selected structures.[a]

St 1CD+3A				TPT			
DNA	C9-CH_2	NMe	H11	H12	18-CH_2	19-CH_3	17-CH_2
H8G1	○	○	○	○			○
H1′G1		○	○	○			○
H3′G1			○				
H4′G1			○	○			○
H5′,H5″G1	○	○	●	○			○
H1′C2							
H4′C2							
H5′,H5″C2							
H6C8	○	○	○				○
H1′C8	○	○				○	○
H2′,H2″C8	●	○	○			○	●

St 1CD+4AB				TPT			
DNA	C9-CH_2	NMe	H11	H12	18-CH_2	19-CH_3	17-CH_2
H8G1	○	○	○	○			○
H1′G1			○	○	●	●	●
H3′G1			○			○	
H4′G1			○	○	●	○	●
H5′,H5″G1	○	○	●	○	○	○	●
H1′C2						○	
H4′C2					○	●	
H5′,H5″C2					○	●	
H6C8	○	○	○	○			○
H1′C8			○	○	○	○	○
H2′,H2″C8	○	○	●	●		○	●

St 2AB+3A				TPT			
DNA	C9-CH_2	NMe	H11	H12	18-CH_2	19-CH_3	17-CH_2
H8G1	○	○	○	○			○
H1′G1	●	●	○				○
H3′G1		○					
H4′G1	○	●	○				○
H5′,H5″G1	○	○	○				○
H1′C2		○					
H4′C2		●					
H5′,H5″C2		●					
H6C8	○	○	○		○	○	●
H1′C8	○	○					
H2′,H2″C8	●	○	○				●

St 2AB+4AB				TPT			
DNA	C9-CH_2	NMe	H11	H12	18-CH_2	19-CH_3	17-CH_2
H8G1	○	○	○	○		○	○
H1′G1	●	●	○	○	●	●	●
H3′G1		○				○	
H4′G1	○	●	○		●	○	●
H5′,H5″G1	○	○	○		○	○	●
H1′C2		○				○	
H4′C2		●			○	●	
H5′,H5″C2		●			○	●	
H6C8	○	○	○	○	○	○	●
H1′C8		○	○	○		○	
H2′,H2″C8	○	○	●	●		○	●

[a] See footnotes for Table 4.

complex, both of TPT on DNA and of DNA on TPT, and these are presented in Figure 6. The results confirm that stacking against the terminal base pair is the major binding mode, and that the St1 geometry does not contribute in any significant way, since its predicted chemical shift patterns (based on ring current effects) do not match the experimentally observed shifts. From the chemical shift changes of the DNA bases it is clear that St2 must be involved, since this is the only model that adequately reproduces observed downfield chemical shift changes on C8. St3A gives a poor match to the experimentally observed shifts on both G1 and C8, and cannot therefore constitute a large part of the conformational ensemble. The chemical shift changes on TPT match St4 better than St2 or St3. Overall, the chemical shift changes therefore agree well with the NOEs in implicating a combination of St2 and St4 as the major structural families.

In summary, we have shown here that TPT binds parallel to the face of the terminal GC pair and that it does so in several different conformations. The methodology presented here is likely to be of general applicability to binding in multiple conformations, particularly in DNA complexes. The result is relevant to any model of nick binding as long as TPT binds against the face of the DNA duplex. In support of this reasoning, we note that in the X-ray study of the ternary DNA/TPT/TopoI complex, TPT was found to intercalate between the $-1/+1$ base pairs, parallel to the face of the base pairs and exactly in the St4 conformation as found in this work. Furthermore, the binding constant in the mM range established in this study may be viewed as reflecting the contribution of the DNA/TPT binding to the overall TPT binding energy in a ternary complex.

Conclusion

An NMR study was undertaken in order to evaluate the binding constant and mode of binding of the camptothecin family drugs CPT and TPT to the DNA octamers $d(GCGTACGC)_2$ and $d(GCGATCGC)_2$. All the results indicate binding of the TPT lactone form, and chemical shift changes show preference of TPT binding to the terminal G1 unit rather than to internal bases. The drug is in fast exchange, and multi-site exchange has been observed and modelled. The carboxylate form of TPT interacts more weakly than the lactone form with DNA.

Intermolecular NOE effects between the DNA oligomer and TPT were observed for the first time, at pH 5 and 3 °C.

The observed cross-peaks cannot be reconciled with a single TPT/DNA complex structure, which suggests a model of a limited number of conformations in fast exchange. MD calculations were therefore performed of the stacking interaction of TPT against the terminal G1–C8 base pair with the use of four starting structures. The use of a small number of experimental restraints as tethers yielded ten MD trajectories (Table 4), and free energy, computed by the MM-PBSA method, was used as a criterion in selecting the trajectories contributing to the conformational space. Ring current effects were calculated for the complexes. These calculations support a combination of two of the starting geometries, St2 and St4, as good fits to the experimentally observed NOE and chemical shift effects. The latter geometry is found in a crystal structure of a TPT/DNA/TopoI ternary complex.

In our model study, camptothecin family drugs bind to DNA duplexes in at least two different orientations, which by implication may both be involved in binding to nicked DNA in vivo. As the binding is weak, the results presented should aid understanding of the inhibitory action of TPT at a molecular level and the design of novel analogues.

Experimental Section

Purification of DNA oligomers: The oligonucleotides d(GCGTACGC)$_2$ and d(GCGATCGC)$_2$ were purchased from Integrated DNA Technologies, Inc. and were purified by ion-exchange chromatography on a HiTrap-Q column (Pharmacia Biotech) by gradient elution with ammonium bicarbonate solution (0.1 M–0.8 M) and desalted on Sephadex G-10. TPT was used as obtained from Glaxo SmithKline. CPT was purchased from Sigma and used without any treatment.

UV experiments: Octamer d(GCGATCGC)$_2$ (1.87 mM, 500 μL) in TPT stock solution (0.1 mM) in a phosphate buffer (50 mM NaCl, 50 mM K_3PO_4, pH 5) in D_2O was placed in a 0.2 cm quartz cell. Increments of 50 μL were removed and replaced by the stock TPT solution. Experiments were performed at 24 °C with a Varian Cary UV/VIS spectrophotometer, and absorbance changes were monitored at 382 nm. The overall association constant for the equilibrium [Eq. (1)].

$$\mathrm{DNA} + \mathrm{TPT} \rightleftharpoons \mathrm{DNA}\cdot\mathrm{TPT} \tag{1}$$

is defined as [Eq. (2)]:

$$K_a = \frac{[\mathrm{DNA}\cdot\mathrm{TPT}]}{[\mathrm{DNA}]\cdot[\mathrm{TPT}_i]} \tag{2}$$

where [DNA·TPT] represents the concentration of DNA bound drug, [DNA] represents the concentration of free DNA, and [TPT$_i$] accounts for the sum of all free TPT species (unbound to DNA). The UV absorbance change is described by Equation (3).[20]

$$\frac{\Delta A}{l} = \frac{[\mathrm{TPT}_i]\cdot K_a\cdot\Delta\varepsilon\cdot[\mathrm{DNA}]}{1 + K_a\cdot[\mathrm{DNA}]} \tag{3}$$

where $\Delta A = A - A_0$ is the difference between the measured absorbance and that for neat TPT, l stands for the cell width, and $\Delta\varepsilon = \varepsilon_{\mathrm{DNA\cdot TPT}} - \varepsilon_{\mathrm{DNA}} - \varepsilon_{\mathrm{TPT}}$ is the UV molar absorptivity change. The free DNA concentration [DNA] is given by Equation (4).

$$[\mathrm{DNA}] = \frac{K_a\cdot[\mathrm{TPT}_i] - K_a\cdot[\mathrm{DNA}_0] + 1 - \sqrt{(K_a\cdot[\mathrm{TPT}_i] - K_a\cdot[\mathrm{DNA}_0] + 1)^2 + 4\cdot K_a\cdot[\mathrm{DNA}_0]}}{-2\cdot K_a} \tag{4}$$

[TPT$_i$] can be related to [TPT$_0$] (allowing for self-association) by Equations (5) and (6).

$$[\mathrm{TPT}_i] = \frac{[\mathrm{TPT}]}{1 - K_a^{\mathrm{TPT}}\cdot[\mathrm{TPT}]} \tag{5}$$

$$[\mathrm{TPT}] = [\mathrm{TPT}_0]\cdot\left(\frac{2}{1 + \sqrt{4\cdot K_a^{\mathrm{TPT}}\cdot[\mathrm{TPT}_0] + 1}}\right)^2 \tag{6}$$

where K_a^{TPT} is previously determined by NMR, [TPT] is the concentration of TPT monomer, and [TPT$_0$] and [DNA$_0$] are total concentrations of TPT and DNA, respectively.

Fluorescence spectroscopy: Steady-state fluorescence spectra were obtained on a Shimadzu RF-5000 fluorimeter fitted with a thermostatted cuvette compartment. Aliquots of DNA oligomer were added to a 1 cm (2 mL) cuvette containing TPT and a magnetic stirrer, and the fluorescence intensity was measured. In experiments at pH 6.3, the initial TPT solution was 10.1 μM in phosphate buffer (50 mM NaCl, 50 mM K_3PO_4, pH 6.3), and the stock solution of DNA was prepared in the TPT stock solution, in order to keep the TPT concentration constant throughout the titration with DNA. The titration resulted in the following concentrations of DNA: 2.12, 6.29, 16.4, 26.0 and 37.85 μM. The UV spectrum of the stock TPT solution showed bands at 382 nm and 414 nm, which were used for excitation. Quenching of the TPT fluorescence was observed only on excitation of the 382 nm band. Experiments at pH 7.8 were performed in the same way, with use of a starting TPT concentration of 11.1 μM. The excitation bands were at 346 and 410 nm.

NMR sample preparation: Two samples were prepared by dissolving the purified and lyophilized octamer in H_2O/D_2O (9:1 *v/v*) containing K_3PO_4 (38 mM) and NaCl buffer (38 mM) at 13 °C (sample 1) and in D_2O containing K_3PO_4 (50 mM) and NaCl (50 mM) at 30 °C (sample 2). No EDTA was added to the samples, which were purified from paramagnetic impurities on a Chelex 100 column (Bio-Rad). Both samples contained TSP-d_4, to monitor the changes of chemical shifts, and were at pH 6. The samples examined in H_2O and D_2O were 1.13 and 1.25 mM in single-strand oligonucleotide, respectively. During the titration experiment, after a DNA/TPT ratio of 1:1 had been reached in sample 1 the pH was changed to 5 to increase the solubility of TPT and the titration was continued until the DNA/TPT ratio was 1:2.5. Concentrations were measured by UV absorption.

NMR experiments

Self-association of TPT: The concentration dependence of TPT chemical shifts was obtained from two experiments. In the first, a 1.3 mM solution of TPT in phosphate buffer (D_2O, 50 mM K_3PO_4, 50 mM NaCl) at pH 6 was diluted stepwise with the same buffer by factors of two down to 0.062 mM. In the second experiment, aliquots of a stock solution of TPT in D_2O (24.4 mM, pH 4.35) were added to a starting solution of 0.91 mM TPT in phosphate buffer at pH 6, up to 7 mM. Since the solubility at pH 6 is lower than in pure D_2O, we measured the concentration in the final additions from the integral of added TSP. The combined data from both experiments were used for evaluation of the association constant by the isodesmic model,[10] which assumes that TPT associates to form stacks, with a single self-association constant K_a^{TPT}. The data from the dilution experiments were used to fit Equation (7).[21]

$$\Delta\delta_{\mathrm{obs}} = \Delta\delta_{\max}\cdot K_a^{\mathrm{TPT}}\cdot[\mathrm{TPT}_0]\cdot\left(\frac{2}{1 + \sqrt{4\cdot K_a^{\mathrm{TPT}}\cdot[\mathrm{TPT}_0] + 1}}\right)^2 \tag{7}$$

where $\Delta\delta_{\mathrm{obs}} = \delta_{\mathrm{mon}} - \delta_{\mathrm{obs}}$ means the change in observed average chemical shift and $\Delta\delta_{\max}$ refers to the maximal chemical shift change between monomer and oligomer.

Gradient spin diffusion experiments: One-dimensional pulsed field gradient diffusion experiments[22] were run in D_2O solution with weak presaturation of the water signal. The reference sample for CPT was composed of D_2O (400 μL), stock solution of CPT in [D_6]DMSO (20 μL) and of neat [D_6]DMSO (80 μL) to dissolve all CPT. The sample of CPT with DNA (d(GCGTACGC)$_2$) was run in D_2O (400 μL), [D_6]DMSO (60 μL) plus NaCl (38 mM), with use

of DNA (1.4 mM) and CPT (1.15 mM) from a stock solution in [D$_6$]DMSO (40 μL). Diffusion experiments were run on a Bruker DRX 500 MHz spectrometer. The FIDs were acquired over 12500 Hz with a 90° pulse width, with use of 0.6 s acquisition, and a 1 s delay after each of 64 scans. A sine-shaped gradient pulse was incremented from 0 to 45 G cm^{-1}, and the interval between gradients was 12 ms.

DNA/TPT titrations: A 0.466 μL solution of 5.8 mM duplex DNA (d(GCGATCGC)$_2$) in a 0.1 mM stock solution of TPT at pH 6 was placed in a 4 mm NMR tube, and 0.128 μL of the solution were removed and replaced with the same volume of a stock 0.1 mM TPT solution, repetitively in 20 steps. Chemical shifts were measured at each step from NOESY and TOCSY spectra, or from 1D spectra where possible. The dissociation constant is given by Equation (8).

$$K_d = \frac{[DNA]\,[TPT_i]}{[DNA \cdot TPT]} = 1/K_a \quad (8)$$

For the titration experiment, two approaches for K_d evaluation from chemical shifts can in principle be attempted, assuming that the TPT is in fast exchange with DNA.[9c] In the first one, the chemical shifts of DNA are used, and in the latter, those of the TPT. The first way will not work in the present case because a large concentration of TPT is required to sample the full range of chemical shift changes, and such high TPT concentrations are not experimentally accessible. Therefore the more reliable approach in this case is the use of the shifts induced on TPT resonances by complexation with DNA.

The concentration of TPT bound to DNA is given by Equation (9).[21]

$$[DNA \cdot TPT] = \frac{K_d + [TPT_i] + [DNA_i] - \sqrt{(K_d + [TPT_i] + [DNA_i])^2 - 4 \cdot [TPT_i] \cdot [DNA_i]}}{2} \quad (9)$$

from which K_d is derived from the experimental measurements of $\Delta\delta_{obs}$ with Equation (10)

$$\Delta\delta_{obs} = (\Delta\delta_{max} - \Delta\delta_{max}^{corr})[DNA \cdot TPT]/[TPT_i] \quad (10)$$

Here, [DNA$_i$] is the sum of all free DNA species (unbound to TPT), [TPT$_i$] represents the sum of all free TPT species (unbound to DNA), $\Delta\delta_{obs} = \delta_{obs} - \delta_{TPT}$, δ_{TPT} is the TPT chemical shift in the absence of DNA, and δ_{obs} means the chemical shift of TPT at different DNA concentrations. $\Delta\delta_{max}$ refers to the maximum chemical shift change between TPT and TPT·DNA, $\Delta\delta_{max}^{corr}$ ($\Delta\delta_{max}$ in Table 1) is the correction of chemical shift of TPT$_i$ for the self-association process, and [DNA$_i$] can be related to [DNA$_0$] through Equations (11) and (12).

$$[DNA_i] = \frac{[DNA]}{1 - K_a^{DNA} \cdot [DNA]} \quad (11)$$

$$[DNA] = [DNA_0] \cdot \left(\frac{2}{1 + \sqrt{4 \cdot K_a^{DNA} \cdot [DNA_0] + 1}} \right)^2 \quad (12)$$

where K_a^{DNA} is the self-association constant in the isodesmic model of DNA self-association, [DNA] is the concentration of DNA monomer, and [DNA$_0$] is the total concentration of DNA. The K_d value allows for DNA and TPT self-association. However, neglect of the TPT or DNA self-association constant has only a marginal effect on the true DNA/TPT K_d value (Table 2). For this reason we have neglected calculation of the even smaller effect of the influence of DNA/TPT binding on the value of TPT self-association.

NOESY spectra:[23] NOESY spectra in H_2O and D_2O were recorded in phase-sensitive mode[24] on a Varian INOVA 500 MHz spectrometer, with 4096 (H_2O sample) and 2048 (D_2O sample) data points in F_2, 64 scans for each of 512×2 increments in F_1, a 250 ms mixing time and a 2 s delay before each scan. Spectra were apodised in both dimensions by use of a squared cosine bell. For the sample in H_2O, linear prediction was applied in the F_1 dimension to extend the data twice, with zero-filling to yield 4096 data points in both dimensions. A binomial sequence was used to suppress the solvent resonance in the H_2O sample, and simple low-power presaturation was applied in the D_2O sample. To minimize zero quantum coherence peaks a small random variation in the mixing time between transients and between t_1 increments was used.[25]

TOCSY spectra:[26] TOCSY spectra were acquired in D_2O with a 5500 Hz spectral window in both dimensions, 2048 data points, and 16 transients over 512 increments with relaxation delays of 1.5 s. The mixing times for TOCSY spectra were 20 and 80 ms with a spin-lock field of 8 kHz.

Computational methods

General: All calculations were carried out by use of the AMBER 6.0 program[27] with the PARM99[28] parameter set. The nucleic acid molecules were neutralized by Na^+ cations. The molecules were surrounded by a periodic box of water described by the TIP3P potential[29] extended to a distance of 10 Å from any solute atom. The number of explicit water molecules included in the simulations varied from 2477 to 2545. The force field parameters for TPT were selected by analogy with existing parameters in the force field. Charges were derived by use of the RESP[30] multiconformational charge-fitting procedure. The ab initio electrostatic potential for RESP was calculated with Gaussian98[31] at the HF/6-31G* level of theory, and two low energy conformers of topotecan were used.

Starting structures: As starting structures for simulation of the TPT/d(GCGATCGC)$_2$ complex, the d(GCGA)$_2$ fragment from the d(CGCGAATTCGCG)$_2$ dodecamer[32] was used, its coordinates being obtained from the Nucleic Acid Database[33] (NDB code BDL001, PDB code 1BNA). Topotecan was docked to the front of the d(GCGA)$_2$ quartet parallel to the G-C base pair in all four possible stacking orientations, giving four starting structures as indicated in Scheme 2.

Molecular dynamics: The particle mesh Ewald (PME) method[34] was used to treat long-range electrostatic interactions with a cubic B spline interpolation and a 10^{-5} tolerance for the direct space sum cutoff. A 9 Å cutoff was applied to the nonbonded Lennard–Jones interactions. The SHAKE algorithm was applied to constrain all bonds involving hydrogen atoms with a tolerance of 10^{-5} Å^2, and a 1 fs time step was used in the dynamics simulation. All systems used the same minimization and equilibration protocols. Firstly, the water molecules and counter-ions were minimized for 1000 steps of steepest descent and 4000 of conjugate gradient method with the DNA and topotecan restrained by 10 kcal mol^{-1} Å^{-2} to the initial positions, followed by a second unrestrained minimization. The next steps of the equilibration protocol were 15 ps constant volume dynamics MD with 5 kcal mol^{-1} Å^{-2} restraints on the DNA and topotecan with the system gradually heated from 10 to 300 K with use of the Berendsen coupling algorithm[35] with a coupling parameter of 1 ps. Then, by use of 50 ps constant pressure MD, with 1 ps pressure relaxation time, the density of the system was adjusted close to 1 g cm^{-3}. During a subsequent 35 ps of constant volume and temperature dynamics the restraints on the TPT and three initial DNA base pairs were gradually reduced to 0.1 kcal mol^{-1} Å^{-2}. The restraint on the last A-T base pair was held constant at 10 kcal mol^{-1} Å^{-2} to prevent distortion in the short DNA model molecule. This 10 kcal mol^{-1} Å^{-2} restraint on the A-T base pair was kept during all subsequent equilibration and production MD simulations. The equilibration protocol was ended by a 1 ns MD run. A 200 kcal mol^{-1} rad^{-2} torsional restraint force was gradually applied in each equilibrated system to the (C8-C9, *C*H$_2$-9, *N*-Me$_2$) dihedral angle in TPT, giving additional structures with opposite orientations of the -CH$_2$-NMe$_2$ group after 20 ps MD runs. Next, we applied a re-docking procedure, consisting of 200 ps MD runs with gradually applied distance restraints (10 kcal mol^{-1} Å^{-2} with 4 Å upper bond threshold), followed by a relaxation. Finally, we ran 600 ps MD trajectories, and recorded the coordinates for further analysis every 1 ps during the last 500 ps.

Free energy analysis: Snapshots for calculation of free energies were taken from the MD trajectories. The 100 snapshots were selected at 5 ps intervals from each trajectory and saved with the water and counter-ion molecules removed. The total free energy changes (ΔG_{tot}) were calculated from the molecular mechanics energies (E_{MM}), and the solvation free energies (G_{sol}).[36] The entropic contribution ($T\Delta S$) was omitted because of the high inaccuracy of accessible methods for its calculation, as the computed entropy vastly exceeds the expected free energy change [Eq. (13)].[37]

$$\Delta G_{tot} = \Delta E_{MM} + \Delta G_{sol} \quad (13)$$

Since all resulting structures have the same mode of binding—that is, stacking to the termini GC base pair—and the DNA structure is not significantly changed due to binding, one can anticipate that the entropy change contribution, $T\Delta S$, should be similar for all complexes in the conformational ensemble. Therefore we ignore the entropy contribution below.

The E_{MM} energies were calculated from internal energies (E_{int}), van der-Waals interaction energies (E_{vdW}), and electrostatic energies (E_{elec}), by use of the Anal module from the AMBER 6.0 package with the same force field and parameter sets as in the MD simulations, but with no cutoff for non-bonded interactions [Eq. (14) and (15)]:

$$E_{MM} = E_{int} + E_{vdW} + E_{elec} \quad (14)$$

$$E_{int} = E_{bond} + E_{angl} + E_{dih} \quad (15)$$

The internal energies (E_{int}) derive from deviations of the bonds (E_{bond}), angles (E_{angl}), and dihedral angles (E_{dih}) from their equilibrium values.

The solvation free energies (G_{solv}) were estimated from the electrostatic solvation energies (G_{PB}) and the nonpolar solvation energies (G_{npol}) [Eq. (16)].

$$G_{solv} = G_{PB} + G_{npol} \quad (16)$$

The electrostatic contribution to the solvation free energies (G_{PB}) was calculated with the DelPhi program[38] by use of the finite difference Poisson–Boltzmann (FDPB) method.[39] The atomic radii were taken from the PARSE parameter set, and the dielectric boundary is defined by use of a probe radius of 1.4 Å, and a grid spacing of 0.5 Å/grid with the solute occupying 50% of the lattice. The boundary potentials were set to the sum of the Debye–Hückel values. A total of 300 linear iterations followed by 1000 nonlinear iterations was performed for each snapshot.

The nonpolar contribution to the solvation free energies (G_{npol}) was estimated as in Equation (17).

$$G_{npol} = \gamma_{SASA} + b \quad (17)$$

where $\gamma = 0.00542\ \text{kcal}\,\text{Å}^{-2}$, $b = 0.92\ \text{kcal}\,\text{mol}^{-1}$,[40] and SASA is the solvent-accessible surface area, which was estimated with an algorithm implemented in the MSMS software.[41] A solvent probe radius of 1.4 Å and PARSE atomic radii values were used.

Back-calculations of NOE effects:[42] NOE effects were calculated with the approximation that correlation times in the DNA/TPT complex are the same for all nuclei, and with neglect of any exchange and motion effects derived from complexation. The NOEs were calculated for each snapshot structure taken from the MD simulations, with use of the cytosine H5–H6 cross-peak volumes for reference, and reported as the average over the trajectory [Eq. (18)].

$$\bar{\eta} = \frac{\sum_i 100\,\% \cdot \frac{r_i^{-6}}{r_0^{-6}}}{N} \quad (18)$$

where $\bar{\eta}$ is the percentage of calculated average NOE compared to the H5–H6 cytosine protons, r_i is the distance between observed protons in i snapshot structure for the total number of N structures and r_0 is the reference distance of 2.47 Å between the H5–H6 cytosine protons. When protons from a rapidly rotating methyl group are involved in an interaction, the expression r^{-6} was replaced by $\langle r^{-3}\rangle^2$. The calculated average NOE effects are reported as small when they exceed 1% and as large when they exceed 15% of the reference H5–H6 cytosine NOE.

Chemical shift calculations: Ring-current effects were calculated with a modified version of the program TOTAL,[43] which uses the Haigh–Mallion method.[44] The DNA bases had ring current intensity factors of 1.0 (G 5-m ring), 0.51 (G 6-m ring) and 0.37 (C ring),[45] while the three aromatic-like rings of TPT each had factors of 0.8. Shifts were calculated for each snapshot of the trajectory, as described above, and averaged. For the DNA octamer shifts in the 1:1 complex, calculated shifts were reduced by a factor of 2.5, because TPT can bind equally well at either end (which will produce 0.5 binding occupancy at each end, and therefore reduce shifts by a factor of two), and because of TPT aggregation, which will further reduce the effective concentration of TPT.

Acknowledgement

The authors thank GlaxoSmithKline for a generous gift of TPT. Help from Dr W. Koźmiński, Warsaw University, is gratefully acknowledged. Thanks are also expressed to Dr. N. Sadlej-Sosnowska for discussion of spectrophotometric data and Ms K. Zakrzewska for help in preparing the UV experiments. We also wish to thank the Danish Instrument Center for NMR Spectroscopy of Biological Molecules at Carlsberg Laboratory for the use of the Varian 800 MHz spectrometer.

[1] a) A. N. Lane, *Methods Enzymol.* **2001**, *340*, 252–281; b) M. A. Keniry, R. H. Shafer, *Methods Enzymol.* **1995**, *261*, 575–604; c) M. S. Searle, *Progr. Nucl. Magn. Reson. Spectrosc.* **1993**, *25*, 403–480.

[2] a) H.-J. Schneider, F. Hacket, V. Rüdiger, H. Ikeda, *Chem. Rev.* **1998**, *98*, 1755–1786; b) S. S. Wijmenga, M. Kruithof, C. W. Hilbers, *J. Biomol. NMR* **1997**, *10*, 337–350.

[3] a) F. Zunino, G. Pratesi, *Expert Opin. Invest. Drugs* **2004**, *13*, 269–284; b) J. F. Pizzolato, L. B. Saltz, *Lancet* **2003**, *361*, 2235–2242; c) H.-K. Wang, S. L. Morris-Natschke, K.-H. Lee, *Med. Res. Rev.* **1997**, *17*, 367–425.

[4] a) L. P. Rivory, J. Robert, *Bull. Cancer* **1995**, *82*, 265–285; b) L. F. Liu, P. Duann, C.-T. Lin, P. D'Arpa, J. X. Wu, *Ann. N. Y. Acad. Sci.* **1996**, *803*, 44–49; c) C. H. Takimoto, J. Wright, S. G. Arbuck, *Biochim. Biophys. Acta* **1998**, 107–119; d) W. J. Slichenmyer, E. K. Rowinsky, R. C. Donehower, S. H. Kaufmann, *J. Natl. Cancer Inst.* **1993**, *85*, 271–291; e) M. C. Wani, A. W. Nicholas, M. E. Wall, *J. Med. Chem.* **1987**, *30*, 2317–2319; f) C. Jaxel, K. W. Kohn, M. C. Wani, M. E. Wall, Y. Pommier, *Cancer Res.* **1989**, *49*, 1465–1469; g) R. P. Hertzberg, M. J. Caranfa, S. M. Hecht, *Biochemistry* **1989**, *28*, 4629–4638; h) R. P. Hertzberg, M. J. Caranfa, K. G. Holden, D. R. Jakas, G. Gallagher, M. R. Mattern, S.-M. Mong, J. O. Bartus, R. K. Johnson, W. D. Kingsbury, *J. Med. Chem.* **1989**, *32*, 715–720; i) Y. Pommier, G. Kohlhagen, K. W. Kohn, F. Leteurtre, M. C. Wani, M. E. Wall, *Proc. Natl. Acad. Sci. USA* **1995**, *92*, 8861–8865.

[5] a) A. Tanizawa, K. W. Kohn, G. Kohlhagen, F. Leteurtre, Y. Pommier, *Biochemistry* **1995**, *34*, 7200–7206; b) R. T. Crow, D. M. Crothers, *J. Med. Chem.* **1992**, *35*, 4160–4164.

[6] a) B. L. Staker, K. Hjerrild, D. Feese, C. A. Behnke, A. B. Burgin, Jr., L. Stewart, *Proc. Natl. Acad. Sci. USA* **2002**, *99*, 15387–15392; b) L. Stewart, M. R. Redinbo, X. Y. Qiu, W. G. J. Hol, J. J. Champoux, *Science* **1998**, *279*, 1534–1541; c) M. R. Redinbo, L. Stewart, P. Kuhn, J. J. Champoux, W. G. J. Hol, *Science* **1998**, *279*, 1504–1513.

[7] D. Z. Yang, J. T. Strode, H. P. Spielmann, A. H-J. Wang, T. G. Burke, *J. Am. Chem. Soc.* **1998**, *120*, 2979–2980.

[8] S. Yao, D. Murali, P. Seetharamulu, K. Haridas, P. N. V. Petluru, D. G. Reddy, F. H. Hausheer, *Cancer Res.* **1998**, *58*, 3782–3786.

[9] a) J.-Sh. Chen, R. B. Shirts, *J. Phys. Chem.* **1985**, *89*, 1643–1646; b) H. K. S. Tan, *J. Chem. Soc. Faraday Trans.* **1994**, *90*, 3521–3525; c) L. Fielding, *Tetrahedron* **2000**, *56*, 6151–6170.

[10] N. J. Baxter, M. P. Williamson, T. H. Lilley, E. Haslam, *J. Chem. Soc. Faraday Trans.* **1996**, *92*, 231–234.

[11] S. Streltsov, V. Oleinikov, M. Ermishov, K. Mochalov, A. Sukhanova, Y. Nechipurenko, S. Grokhovsky, A. Zhuze, M. Pluot, I. Nabiev, *Biopolymers* **2003**, *72*, 442–454.

[12] A. R. Waldeck, P. W. Kuchel, A. J. Lennon, B. E. Chapman, *Progr. Nucl. Magn. Reson. Spectrosc.* **1997**, *30*, 39–68.

[13] a) A. Gafni, Y. Cohen, *J. Org. Chem.* **1997**, *62*, 120–125; b) O. Mayzel, Y. Cohen, *J. Chem. Soc. Chem. Commun.* **1994**, 1901–1902.

[14] S. Streltsov, A. Sukhanova, A. Mikheikin, S. Grokhovsky, A. Zhuze, I. Kudelina, V. Mochalov, J.-C. Jardillier, I. Nabiev, *J. Phys. Chem. B* **2001**, *105*, 9643–9652.

[15] G. C. K. Roberts, *Curr. Opin. Biotechnol.* **1999**, *10*, 42–47.

[16] a) Y. Fan, J. N. Weinstein, K. W. Kohn, L. M. Shi, Y. Pommier, *J. Med. Chem.* **1998**, *41*, 2216–2226; b) X. Wang, X. Zhou, S. M. Hecht, *Biochemistry* **1999**, *38*, 4374–4381; c) J. E. Kerrigan, D. S. Pilch, *Biochemistry* **2001**, *40*, 9792–9798; d) G. S. Laco, J. R. Collins, B. T. Luke, H. Kroth, J. M. Sayer, D. M. Jerina, Y. Pommier, *Biochemistry* **2002**, *41*, 1428–1435.
[17] M. P. Williamson, J. P. Waltho, *Chem. Soc. Rev.* **1992**, *21*, 227–236.
[18] S. X. Yan, R. Shapiro, N. E. Geacintov, S. Broyde, *J. Am. Chem. Soc.* **2001**, *123*, 7054–7066.
[19] M. J. Blackledge, R. Brüschweiler, C. Griesinger, J. M. Schmidt, P. Xu, R. R. Ernst, *Biochemistry* **1993**, *32*, 10960–10974.
[20] K. A. Connors, *Binding Constants*, Wiley, New York, **1987**, Chapter 4.
[21] A. J. Charlton, N. J. Baxter, M. L. Khan, A. J. G. Moir, E. Haslam, A. P. Davies, M. P. Williamson, *J. Agric. Food Chem.* **2002**, *50*, 1593–1601.
[22] A. S. Altieri, D. P. Hinton, R. A. Byrd, *J. Am. Chem. Soc.* **1995**, *117*, 7566–7577.
[23] J. Jeener, B. H. Meier, P. Bachmann, R. R. Ernst, *J. Chem. Phys.* **1979**, *71*, 4546–4553.
[24] a) G. Bodenhausen, H. Kogler, R. R. Ernst, *J. Magn. Reson.* **1984**, *58*, 370–388; b) D. J. States, R. A. Haberkorn, D. J. Ruben, *J. Magn. Reson.* **1982**, *48*, 286–292.
[25] D. Neuhaus, M. P. Williamson, *The Nuclear Overhauser Effect in Structural and Conformational Analysis*, VCH Publishers, New York, **1989**, Chapter 8.4.
[26] a) L. Braunschweiler, R. R. Ernst, *J. Magn. Reson.* **1983**, *53*, 521–528; b) C. Griesinger, G. Otting, K. Wüthrich, R. R. Ernst, *J. Am. Chem. Soc.* **1988**, *110*, 7870–7872.
[27] D. A. Pearlman, D. A. Case, J. C. Caldwell, G. L. Seibel, U. C. Singh, P. Weiner, P. A. Kollman, *AMBER Program Package*; **1991**, UCSF; San Francisco, CA.
[28] J. M. Wang, P. Cieplak, P. A. Kollman, *J. Comput. Chem.* **2000**, *21*, 1049–1074.
[29] W. L. Jorgensen, J. Chandrasekhar, J. D. Madura, R. W. Impey, M. L. Klein, *J. Chem. Phys.* **1983**, *79*, 926–935.
[30] C. I. Bayly, P. Cieplak, W. D. Cornell, P. A. Kollman, *J. Phys. Chem.* **1993**, *97*, 10269–10280.
[31] Gaussian 98, M. J. Frisch, G. W. Trucks, H. B. Schlegel, G. E. Scuseria, M. A. Robb, J. R. Cheeseman, V. G. Zakrzewski, J. A. Montgomery, Jr., R. E. Stratmann, J. C. Burant, S. Dapprich, J. M. Millam, A. D. Daniels, K. N. Kudin, M. C. Strain, O. Farkas, J. Tomasi, V. Barone, M. Cossi, R. Cammi, B. Mennucci, C. Pomelli, C. Adamo, S. Clifford, J. Ochterski, G. A. Petersson, P. Y. Ayala, Q. Cui, K. Morokuma, D. K. Malick, A. D. Rabuck, K. Raghavachari, J. B. Foresman, J. Cioslowski, J. V. Ortiz, A. G. Baboul, B. B. Stefanov, G. Liu, A. Liashenko, P. Piskorz, I. Komaromi, R. Gomperts, R. L. Martin, D. J. Fox, T. Keith, M. A. Al-Laham, C. Y. Peng, A. Nanayakkara, C. Gonzalez, M. Challacombe, P. M. W. Gill, B. G. Johnson, W. Chen, M. W. Wong, J. L. Andres, M. Head-Gordon, E. S. Replogle, J. A. Pople, Gaussian, Inc., Pittsburgh PA, **1998**.
[32] H. R. Drew, R. M. Wing, T. Takano, C. Broka, S. Tanaka, K. Itakura, R. E. Dickerson, *Proc. Natl. Acad. Sci. USA* **1981**, *78*, 2179–2183.
[33] H. M. Berman, W. K. Olson, D. L. Beveridge, J. Westbrook, A. Gelbin, T. Demeny, S.-H. Hsieh, A. R. Srinivasan, B. Schneider, *Biophys. J.* **1992**, *63*, 751–759.
[34] U. Essmann, L. Perera, M. L. Berkowitz, T. Darden, H. Lee, L. G. Pedersen, *J. Chem. Phys.* **1995**, *103*, 8577–8593.
[35] H. J. C. Berendsen, J. P. M. Postma, W. F. van Gunsteren, A. DiNola, J. R. Haak, *J. Chem. Phys.* **1984**, *81*, 3684–3690.
[36] a) B. Jayaram, D. Sprous, M. A. Young, D. L. Beveridge, *J. Am. Chem. Soc.* **1998**, *120*, 10629–10633; b) T. E. Cheatham, J. Srinivasan, D. A. Case, P. A. Kollman, *J. Biomol. Struct. Dyn.* **1998**, *16*, 265–280; c) P. A. Kollman, I. Massova, C. Reyes, B. Kuhn, S. H. Huo, L. Chong, M. Lee, T. Lee, Y. Duan, W. Wang, O. Donini, P. Cieplak, J. Srinivasan, D. A. Case, T. E. Cheatham, *Acc. Chem. Res.* **2000**, *33*, 889–897.
[37] a) J. Srinivasan, T. E. Cheatham, P. Cieplak, P. A. Kollman, D. A. Case, *J. Am. Chem. Soc.* **1998**, *120*, 9401–9409; b) V. Tsui, D. A. Case, *J. Phys. Chem. B* **2001**, *105*, 11314–11325.
[38] A. Nicholls, K. A. Sharp, B. Honig, *DelPhi*, Department of Biochemistry and Molecular Biophysics, Columbia University, New York, **1990**.
[39] K. A. Sharp, B. Honig, *J. Phys. Chem.* **1990**, *94*, 7684–7692.
[40] D. Sitkoff, K. A. Sharp, B. Honig, *J. Phys. Chem.* **1994**, *98*, 1978–1988.
[41] M. F. Sanner, A. J. Olson, J. C. Spehner, *Biopolymers* **1996**, *38*, 305–320.
[42] D. Neuhaus, M. P. Williamson, The Nuclear Overhauser Effect in Structural and Conformational Analysis, Wiley, New York, **1989**, p. 1.
[43] M. P. Williamson, T. Asakura, *J. Magn. Reson. Ser. B* **1993**, *101*, 63–71.
[44] C. W. Haigh, R. B. Mallion, *Progr. Nucl. Magn. Reson. Spectrosc.* **1980**, *13*, 303.
[45] D. A. Case, *J. Biomol. NMR* **1995**, *6*, 341–346.

Received: October 14, 2003
Revised: June 7, 2004
Published online: October 7, 2004

